Chapter 21
2D Methods of Monitoring Exchange

Keith G. Orrell

University of Exeter, Exeter, UK

21.1 INTRODUCTION

The suitability of NMR spectroscopy for monitoring exchange processes of molecules has been realized since the earliest days of the technique. In those formative years, rate processes were studied primarily by their effects on internal resonance frequencies of nuclei (bandshape analysis)[1] or on signal intensities (magnetization transfer experiments).[2,3] The first method relies on exchange processes occurring at frequencies comparable to differences in nuclear resonance frequencies $\Delta\nu_i$, whereas the second approach requires exchange rates to be comparable to spin–lattice relaxation rates R_{1i}. The consequences of such criteria are that bandshape analysis methods are applicable to rather faster rate processes, with pseudo-first-order rate constants k in the range $1-10^4$ s^{-1}, than magnetization transfer methods, where typically k values are in the range $10^{-2}-10^2$ s^{-1}. Such ranges, however, are very imprecise, and depend on the nucleus chosen to monitor the process and the nature of the chemical species itself—for example, whether it is diamagnetic or paramagnetic.

In magnetization transfer experiments, based on the classic work of Forsén and Hoffman,[2,3] nuclei in one of the exchanging sites are labeled by disturbing their energy population distribution, either by selective decoupling, which equalizes their populations (saturation), or by applying a selective 180° pulse, which inverts their populations (inversion). Chemical exchange causes these nuclei to move to one or more different sites, thus introducing a further disturbance to the populations in that site. This leads to a time dependence of populations of exchanging sites, which is reflected in the changing intensities of signals following the perturbing pulse. Measurements of this intensity variation can provide accurate exchange rate data. The method can be made very reliable for two-site exchange,[4] and has been very widely applied. The method can also be generalized for multisite exchange, where it has been shown that for a system of N exchanging sites $^1/_2N(N-1)$ exchange rates and N spin–lattice relaxation rates need to be evaluated.[5] However, this requires many experiments, and this type of problem is far more efficiently handled by two-dimensional experiments,[6–8] which are the subject of this chapter.

Rate processes that cause exchange of magnetization between nuclear sites are many and varied. They range from examples of intermolecular exchange (e.g., ligand or solvent exchange processes) to subtle intramolecular rearrangements between chemically

identical species (e.g., fluxional processes). This chapter presents the basic theory of two-dimensional exchange spectroscopy (EXSY), illustrates the scope and limitations of the technique, and provides examples of its application, employing a variety of different sensor nuclei, to different areas of chemistry.

The focus will be on chemical exchange arising from structural rearrangements of molecules, but the reader is reminded that essentially the same technique is used for studying motional processes as revealed by cross relaxation rather than chemical exchange effects. In this context, the technique is known as two-dimensional NOE spectroscopy, and has been widely exploited[9] (see Chapter 18).

21.2 THEORY AND METHODOLOGY OF 2D EXCHANGE SPECTROSCOPY

The application of 2D NMR for chemical exchange studies was first described by Jeener, Meier, Bachmann, and Ernst.[10] Its theoretical basis was elaborated by Macura and Ernst,[11] and has been the subject of a number of reviews.[12–15]

21.2.1 Basic EXSY Experiment

The fundamental principle of the EXSY experiment is the frequency labeling of the longitudinal magnetization of various sites before exchange occurs, in order that, after exchange, the pathways of magnetization can be traced back to their origins.

The basic pulse sequence is shown in Figure 21.1. A two-spin system of spins A and B, mutually interacting purely through chemical exchange with no cross relaxation, will be considered. Equal concentrations of spins (i.e., $k_{AB} = k_{BA} = k$), equal spin–lattice relaxation rates ($R_1^A = R_1^B = R_1$), and equal transverse relaxation times ($T_2^A = T_2^B = T_2$) will be assumed. After the first 90°_x pulse, the magnetization vectors will evolve in the (x', y') plane in the usual manner of free induction decay (FID) for a period t_1 (evolution time). The total magnetization M^+ is given by

$$M^+ = M_y(t) + iM_x(t) \tag{21.1}$$

If exchange is slow, the effect of lineshape may be neglected, and the two magnetization components are given by

$$M_A^+(t_1) = M_{A0}\exp(i\omega_A t_1 - t_1/T_2) \tag{21.2}$$

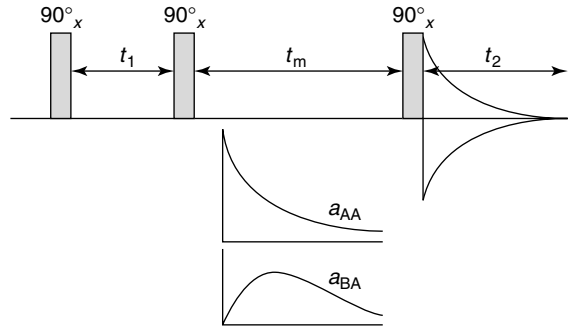

Figure 21.1. Basic EXSY pulse sequence, showing typical variations in the mixing coefficients for diagonal (a_{AA}) and cross (a_{BA}) peaks during the mixing time t_m.

$$M_B^+(t_1) = M_{B0}\exp(i\omega_B t_1 - t_1/T_2) \tag{21.3}$$

where $\omega_{A,B}$ are the effective precession frequences in the rotating frame. When a second 90°_x pulse is applied, the magnetization vectors are tipped into the $-z$ direction, the real components of the transverse magnetization being converted into longitudinal magnetization:

$$M_{AZ}(t_m = 0) = -M_{A0}\cos\omega_A t_1 \exp(-t_1/T_2) \tag{21.4}$$

$$M_{BZ}(t_m = 0) = -M_{B0}\cos\omega_B t_1 \exp(-t_1/T_2) \tag{21.5}$$

The imaginary x components are unaffected by this pulse, and may be destroyed by a field gradient pulse during the mixing time t_m. The t_1-modulated longitudinal components in equations (21.4) and (21.5) migrate from one site to another by chemical exchange, with a rate constant k, while the spin–lattice relaxation attenuates the memory of the initial labeling:

$$\begin{aligned} M_{AZ} = {} & M_{AZ}(t_m = 0)\tfrac{1}{2}[1 + \exp(-2kt_m)]\exp(-t_m R_1) \\ & + M_{BZ}(t_m = 0)\tfrac{1}{2}[1 - \exp(-2kt_m)]\exp(-t_m R_1) \end{aligned} \tag{21.6}$$

$$\begin{aligned} M_{BZ} = {} & M_{AZ}(t_m = 0)\tfrac{1}{2}[1 - \exp(-2kt_m)]\exp(-t_m R_1) \\ & + M_{BZ}(t_m = 0)\tfrac{1}{2}[1 + \exp(-2kt_m)]\exp(-t_m R_1) \end{aligned} \tag{21.7}$$

The final 90°_x pulse converts these longitudinal components into observable magnetization. Double Fourier transformation will produce signals at $(\omega_1, \omega_2) = (\omega_A, \omega_A)$ and (ω_B, ω_B) for nuclei that have not exchanged during the time t_m. Nuclei

that have exchanged sites will produce signals at (ω_A, ω_B) and (ω_B, ω_A). The amplitudes $I_{kl}(t_m)$ of the diagonal and off-diagonal signals depend on the equilibrium magnetizations M_{l0} and on mixing coefficients $a_{kl}(t_m)$, which correspond to the factors in equations (21.6) and (21.7):

$$a_{AA} = a_{BB} = \tfrac{1}{2}[1 + \exp(-2kt_m)]\exp(-t_m R_1) \tag{21.8}$$

$$a_{AB} = a_{BA} = \tfrac{1}{2}[1 - \exp(-2kt_m)]\exp(-t_m R_1) \tag{21.9}$$

In this simple two-site exchange system, the equilibrium magnetizations M_{A0} and M_{B0} are equal, and the exchange rate can be determined from the ratio of diagonal and off-diagonal (cross peak) intensities:

$$\frac{I_{AA}}{I_{AB}} = \frac{a_{AA}}{a_{AB}} = \frac{1 + \exp(-2kt_m)}{1 - \exp(-2kt_m)} \approx \frac{1 - kt_m}{kt_m} \tag{21.10}$$

This intensity ratio is a sensitive function of the length of the mixing time t_m, and care must be taken with the length chosen in order to obtain optimum accuracy of the rate constant. The amplitudes of the diagonal signals decay in biexponential manner with increasing mixing time, whereas the off-diagonal signals first increase owing to exchange and then decrease because of spin–lattice relaxation (see Figure 21.1). The optimal value of t_m corresponds to the region on the graph where the intensity of the cross peak is almost linearly proportional to t_m, and well before it reaches a level where its intensity is more dependent on T_1 than on t_m. It has been shown theoretically[13] that an approximate expression for the optimal value of t_m for an equally populated two-site exchange system is

$$t_m(\text{opt}) \approx (R_1 + 2k)^{-1} \tag{21.11}$$

One of the first reported EXSY spectra is shown in Figure 21.2.[10] It depicts the diagonal and cross-peak signals of the *N*-methyl hydrogens of *N*,*N*-dimethylacetamide, which exhibit exchange due to the slow rotation about the C–N bond in the molecule.

This theory can be extended to general *N*-site exchange when $N \geq 3$ using a matrix formulation. This has been described fully elsewhere,[12–15] and here space permits only a summary. For nuclei in site *j*, the initial 90°_x pulse causes their magnetization to evolve according to

$$M_j = M_{j0}\exp(\mathrm{i}\omega_j t_1 - t_1/T_{2j}) \tag{21.12}$$

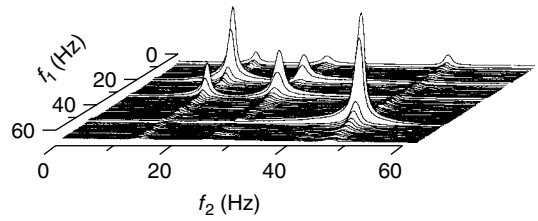

Figure 21.2. Proton EXSY spectrum of *N*,*N*- dimethylacetamide, showing the *N*-methyl exchange cross peaks. Experimental conditions: 128 equidistant t_1 values from 0 to 1016 ms, each FID represented by 256 samples, and a mixing time $t_m = 0.5$ s. Note that diagonal signals go from top left to bottom right.

The second 90°_x pulse, plus a gradient pulse, converts this transverse magnetization to *z* magnetization according to

$$M_{jz}(t_m = 0) = -M_{j0}\exp(\mathrm{i}\omega_j t_1 - t_1/T_{2j}) \tag{21.13}$$

During the mixing period, chemical exchange and longitudinal relaxation affect this magnetization. We define m_j to be the deviation of M_{jz} from its equilibrium value by

$$m_j = M_{jz} - M_{j0} \tag{21.14}$$

The time dependences of these deviations are given by equations of the type

$$\frac{\mathrm{d}m_1}{\mathrm{d}t} = -\left(R_{11} + \sum_l k_{1l}\right) \times m_1 + k_{21}m_2 + \cdots + k_{N1}m_N \tag{21.15}$$

$$\frac{\mathrm{d}m_2}{\mathrm{d}t} = k_{12}m_1 - \left(R_{12} + \sum_l k_{2l}\right) \times m_2 + \cdots + k_{N2}m_N \tag{21.16}$$

$$\vdots$$

$$\frac{\mathrm{d}m_N}{\mathrm{d}t} = k_{1N}m_N + k_{2N}m_2 + \cdots - \left(R_{1N} + \sum_l k_{N1}\right)m_N \tag{21.17}$$

where k_{ij} are the rate constants for exchange from site *i* to site *j*, and R_{1i} are the spin–lattice relaxation rates of nuclei in site *i*. These equations may be written in matrix form as

$$\dot{\boldsymbol{m}} = -\boldsymbol{L}\boldsymbol{m} \tag{21.18}$$

where $\boldsymbol{m}$ is a column matrix whose components are $m_1, m_2, \ldots, m_N$, $\dot{\boldsymbol{m}}$ is the time derivative of $\boldsymbol{m}$, and $\boldsymbol{L}$ is a square $N \times N$ matrix whose off-diagonal elements are $L_{ij} = -k_{ji}$ and whose diagonal elements are $L_{ii} = \sum_l k_{il} + R_{1i}$. This matrix $\boldsymbol{L}$ contains all site-to-site rate constants, and the problem is to relate the elements of $\boldsymbol{L}$ to the signal intensities in an EXSY spectrum. The formal solution is given by

$$\boldsymbol{m}(t_m) = \exp(-\boldsymbol{L}t_m)\boldsymbol{m}(0) \tag{21.19}$$

where $\boldsymbol{m}(0)$ is the column matrix of the deviations $m_j(0)$ at the start of the mixing period.

The explicit expression for the intensity of any EXSY signal (diagonal or off-diagonal) at ω_i along the frequency coordinate ω_2 and at ω_j along ω_1 is given by[13]

$$\begin{aligned} I_{ij}(t_m) &= M_{j0}\exp(-\boldsymbol{L}t_m)_{ij} \\ &= \left(\delta_{ij} - t_m L_{ij} + \tfrac{1}{2}t_m^2 \textstyle\sum_k L_{ik}L_{kj} - \cdots\right) M_{j0} \end{aligned} \tag{21.20}$$

where $\delta_{ij} = 1$ $(i = j)$ or 0 $(i \neq j)$. Equation (21.20) shows that an EXSY spectrum represents a graphical display of the exchange pathways, with cross peaks corresponding to nuclei that exchange sites. Intensities of signals correspond to the exponential of the matrix $\boldsymbol{L}$, allowance being made for the fact that the mathematical convention of a matrix is with the diagonal running from top left to bottom right whereas an EXSY spectral map consists of a diagonal running from bottom left to top right.

21.2.2 Extraction of Rate Data from EXSY Spectra

The complexity of equation (21.20) arises because cross peaks for exchange between sites i and j can arise from both direct exchange $i \rightleftharpoons j$ and indirect exchange, $i \rightleftharpoons k \rightleftharpoons j$. For very short t_m values, the indirect cross peaks vanish, and equation (21.20) simplifies. However, short t_m values cause all cross-peak intensities to be low, so this approach is of limited applicability. Three strategies have been employed to extract reliable rate data from EXSY spectra.

21.2.2.1 Initial Rate Approximation

This involves measuring cross-peak intensities as a function of small values of t_m.[16] Rate constants k_{ij} are determined from the slope of the graph of $I_{ij}(t_m)$ versus $M_{j0}(t_m)$, but the method involves repeating the experiment for a range of mixing times and extrapolating to $t_m = 0$, which is a time-consuming approach.

21.2.2.2 Iterative Analysis

In this method,[17] trial values of k_{ij} and R_{1i} are chosen, and a total magnetization transfer matrix $\boldsymbol{L}$ is constructed. Diagonalization of this yields a signal intensity matrix, which is compared with the experimental intensity array. An iterative fitting is then performed by varying exchange and relaxation rates until a "best fit" is obtained.

21.2.2.3 Direct Matrix Transformation

Unlike the previous method, this approach does not require any prior knowledge of k_{ij} and R_{1i} values, and uses a matrix method for inverting equation (21.20) first presented by Perrin and Gipe.[18] It is based on expressing an EXSY spectrum as an intensity matrix $\boldsymbol{I}$ with elements

$$I_{ij} = p_i \sum_{k=1}^{N} A_{ijk}\exp(\lambda_k t_m) \tag{21.21}$$

where p_i is the relative population of site i, and A_{ijk} and λ_k are constants depending on the experimental conditions. In matrix form,

$$\boldsymbol{I} = \boldsymbol{P}\boldsymbol{J} \tag{21.22}$$

where $\boldsymbol{P}$ is a column matrix of site populations and $\boldsymbol{J}$ is a matrix with elements $\exp(\lambda_k t_m)$. The kinetic matrix $\boldsymbol{K}$ consisting purely of rate constants k_{ij} can be related to the EXSY spectral intensity matrix $\boldsymbol{I}$ by

$$\boldsymbol{I} = \boldsymbol{P}\exp(\boldsymbol{K}t_m) \tag{21.23}$$

Now, $\boldsymbol{J} = \boldsymbol{I}\boldsymbol{P}^{-1}$, and diagonalization of $\boldsymbol{J}$ will generate the array $\exp(\boldsymbol{\Lambda}t_m)$:

$$\boldsymbol{J} = \boldsymbol{X}\exp(\boldsymbol{\Lambda}t_m)\boldsymbol{X}^{-1} \tag{21.24}$$

Taking the natural logarithm of the eigenvalues and dividing by t_m, i.e.,

$$\frac{\ln \boldsymbol{J}}{t_m} = \frac{\boldsymbol{X}\ \ln\exp(\boldsymbol{\Lambda}t_m)\boldsymbol{X}^{-1}}{t_m} \tag{21.25}$$

generates the matrix $\boldsymbol{\Lambda}$.

Finally, matrix multiplication

$$\boldsymbol{X}\boldsymbol{\Lambda}\boldsymbol{X}^{-1} = \boldsymbol{K} \tag{21.26}$$

yields the kinetic matrix $\boldsymbol{K}$, consisting of all rate constants for the multisite process. It should be noted that in this formulation,[19] all off-diagonal elements are positive and diagonal elements negative, in contrast to the kinetic part of the $\boldsymbol{L}$ matrix defined earlier [equation (21.18)].

It is also necessary to include spin–lattice relaxation of nuclei. This can take the form of a relaxation matrix $\boldsymbol{R}$, which when added to $\boldsymbol{K}$ gives the total magnetization transfer matrix $\boldsymbol{L}$:

$$\boldsymbol{L} = \boldsymbol{K} + \boldsymbol{R} \tag{21.27}$$

The matrix $\boldsymbol{R}$ consists of diagonal elements $-R_{1i}$ and off-diagonal elements $-\sigma_{ij} = -R_{ij}$, where these refer to cross-relaxation rates.

In cases where cross-relaxation between nuclei can be neglected, the above procedures have been incorporated into a general computer program.[19] Its input consists of the number of exchanging sites (2–8), the relative populations of each site, spin–lattice relaxation rates, and experimental signal intensities, the latter being measured by integration of appropriate rows of the 2D spectral map, or, preferably, by volume integration. The accuracy of the final rate data depends on the choice of mixing time and on the accuracy of measured signal intensities. Pure absorption mode spectra provide better resolution of closely separated signals than magnitude mode spectra. This can be achieved using time proportional phase incrementation (TPPI), and so this is the recommended procedure for accurate quantitative EXSY studies. The ^{1}H EXSY spectrum of [^{15}N]acetamide using this procedure is shown in Figure 21.3.[20] Both NH signals are doublets [^{1}J(NH) $\approx$ 90 Hz], and exhibit cross peaks due to slow C–N bond rotation. Intensity measurements of all eight signals provided accurate rate and R_1 values for the NH hydrogens. The much weaker cross peaks are due to ^{15}N spin–lattice relaxation occurring during the mixing period.

The assessment of errors in EXSY-based rate constants is an important matter which has received careful consideration.[19,21,22] The choice of mixing time has already been shown to be crucial. In multisite exchanges, it is usually impossible to find a single value of t_m that is optimal for all exchange pathways. Additional cross peaks due to indirect exchanges [equation (21.20)] may then arise if the mixing time is considerably greater than optimal, and so qualitative

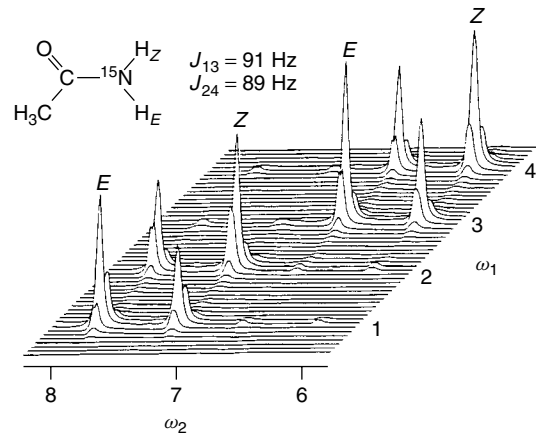

Figure 21.3. Partial phase-sensitive ^{1}H EXSY spectrum of ^{15}N-enriched-acetamide obtained with the TPPI method for $t_m = 400$ ms. A 1k data block and spectral width in ω_2 of 614 Hz were used. A total of 256 t_1 values was used and zero filled to 1k, resulting in a digital resolution of 1.2 Hz point^{-1} in both frequency domains.

interpretations of exchange pathways from EXSY spectra must be made with caution.

21.2.3 Separation of Chemical Exchange and Cross-Relaxation Effects

The theoretical treatment above has neglected cross-relaxation between nuclei; i.e., off-diagonal elements of the matrix $\boldsymbol{R}$ have been assumed to be negligibly small. This is generally valid for intermolecular exchanges and studies of intramolecular exchange using low-abundance sensor nuclei (e.g., ^{13}C). Also, it is often valid for studies of abundant nuclei (e.g., ^{1}H, ^{19}F, and ^{31}P) in small molecules, which can undergo rapid tumbling in solution. For large, slowly tumbling molecules, however, separation of chemical exchange and cross-relaxation rates is essential.

Cross-relaxation rates are given by

$$\sigma_{ij} = \frac{\gamma^4\hbar^2\tau_c}{10r_{ij}^6}\left(\frac{6}{1+4\omega^2\tau_c^2} - 1\right) \tag{21.28}$$

where r_{ij} is the distance between nuclei i and j, and τ_c is the rotational correlation time of the molecule. The r^{-6} dependence provides proximity information, which has been widely exploited in conformational studies of complex molecules.[9] For

small molecules, where τ_c is short, cross-relaxation cross peaks are of opposite sign to diagonal signals, whereas for macromolecules with relatively large τ_c values, cross-relaxation signals are of the same sign as the diagonals. Pure absorption mode (TPPI) spectra, therefore, can in theory distinguish the two cases, but in either case cross-peak intensities may not reflect chemical exchange alone.

Separation of cross relaxation and chemical exchange is most easily achieved by temperature dependence studies, since k_{ij} values increase greatly with temperature whereas σ_{ij} values do not. More recently, new pulse sequences have been suggested for achieving this separation. These include zz-EXSY,[23] an interlayed NOESY/ROESY method,[24] and gradient-enhanced exchange spectroscopy (GEXSY).[25]

21.2.4 One-Dimensional Variants of EXSY

The time required to obtain kinetic data from EXSY experiments can often be considerable, especially if long relaxation delays, long mixing times, and high digital resolution in both dimensions are required. Much time is incurred scanning through the whole range of incremental evolution periods, t_1, yet the majority of rows in the final spectrum do not contain useful information. However, certain t_1 values cannot simply be omitted, since each value contributes to all frequencies through the FID. One method for shortening the experimental time would be to dispense with the t_1 period completely and rely on selective excitation. The feasibility of this approach has been demonstrated for COSY experiments and is known as pseudo-COSY (ψ-COSY).[26] A similar technique has recently been proposed for exchange spectroscopy. It is described as multiplet-selective excitation or MUSEX,[27] and is based on selective excitation of only one nucleus of a coupled system using a typical DANTE pulse.[28]

Another variant uses the normal nonselective pulse sequence and difference spectroscopy.[29] For N-site exchange, data for N evolution times must be collected, measuring each at zero and nonzero mixing times. Difference spectra obtained by subtracting the equilibrium spectrum from spectra recorded both without and with mixing yields exchange information. For a system of three spins A, B, and C, six one-dimensional spectra are measured for three t_1 periods, each without and with mixing. It follows that

$$\begin{bmatrix} A(t_m) - A_0 \\ B(t_m) - B_0 \\ C(t_m) - C_0 \end{bmatrix} = \exp(-\boldsymbol{L}t_m) \begin{bmatrix} A(t_m = 0) - A_0 \\ B(t_m = 0) - B_0 \\ C(t_m = 0) - C_0 \end{bmatrix} \tag{21.29}$$

The matrix $\boldsymbol{L}$ can then be computed by a version of the back transformation method (see 21.2.2.3). Greater accuracy can be achieved if the experiment is performed for more t_1 values than are strictly necessary.[30]

21.2.5 Other Variants of EXSY

In 1989, Jeener, one of the pioneers of 2D NMR and its application to chemical kinetics, returned to this subject by examining the theoretical basis of the bandshapes of EXSY signals.[31] He has shown that the shapes, particularly of off-diagonal signals, provide a clear signature of the chemical exchange process even for a single temperature. Superoperator theory was applied to one- and two-spin exchanging signals. Computation, however, is not trivial, and no obvious advantages of this approach over conventional 1D bandshape analysis or 2D EXSY experiments are apparent at this stage.

In its most general form, the EXSY or NOESY pulse sequence involves three time variables, t_1, t_m, and t_2, Fourier transformation of all of which would lead to three-dimensional spectra. In practice, however, the mixing time t_m is not taken as a time variable, and 2D spectra based on a very limited range of t_m values are usually obtained. An alternative approach is to make t_m proportional to t_1 (i.e., $t_m = \kappa t_1$). The resulting "accordion" technique[32] leads to EXSY-type spectra in which the signals are distorted from their usual shapes, and rate constants need to be extracted from signal widths rather than intensities. This restricts the versatility of the method.

Three-dimensional NMR experiments are now rapidly gaining ground[33] (see Chapter 2). In 3D exchange spectroscopy, two successive exchange processes may be mapped. These may be chemical exchange (EXSY) or cross relaxation in either the laboratory frame (NOESY) or in the rotating frame (ROESY), resulting in such experiments as EXSY–EXSY and NOESY–ROESY. In the context of this chapter, it should be mentioned that a 3D EXSY–EXSY spectrum of heptamethylbenzenonium sulfate (in sulfuric acid) has been obtained,[33]

showing the 1,2-commutation of the methyl group round the ring. It is too early to predict whether such experiments will provide more insight into dynamic processes than can be achieved by 1D and 2D experiments. Dynamic studies of highly complex molecules would appear to be most likely to gain by the extra frequency dimension.

21.3 APPLICATIONS OF EXSY

A few representative examples of EXSY experiments using different sensor nuclei will now be given.

21.3.1 Carbon-13 and Hydrogen-1

In 21.2.3, the separation of chemical exchange and cross-relaxation contributions to cross peak intensities was discussed. This problem does not arise in EXSY spectra of low-abundance nuclei (e.g., ^{13}C), where cross-relaxation effects are negligible, but is a potential problem with abundant nuclei such as ^{1}H. A specific case has been described where the effects of $^{1}H-^{1}H$ cross relaxation have been quantified.[34] In the trinuclear rhenium complex $[Re_3(\mu\text{-}H)_4(CO)_{10}]$, carbonyl scrambling occurs by a concerted mechanism, the kinetics of which can be measured accurately by ^{13}C EXSY. Lower accuracy would be attached to ^{1}H-EXSY-based rates, since one-dimensional selective perturbation data showed that the cross-relaxation rate of a pair of bridging hydrogens was 0.04 s^{-1}, a small but not negligible rate. On the other hand, a combined ^{13}C and ^{1}H EXSY study of the metal migration in the cyclooctatetraene (COT) complexes $[M(CO)_3(\eta^6\text{-COT})]$ (M = Cr or W) produced kinetic data in excellent agreement with each other, indicating that $^{1}H-^{1}H$ cross relaxation in this case was negligible.[35]

21.3.2 Lithium-7

The first ^{7}Li EXSY spectra have recently been produced in connection with a kinetic study of the complex [lithium monobenzo-15-crown-5]$^{+}$ in nitromethane.[36] Mixing times varied between 5 and 100 ms, nine experiments being performed, each requiring 1 h of spectrometer time. Rate data were in close agreement with those measured by bandshape analysis, showing that the EXSY method can be applied with confidence to systems such as cryptands, where exchange is too slow for bandshape treatment.

21.3.3 Boron-11

The well-known redistribution reactions of boron trihalide mixtures have been examined by ^{11}B EXSY.[37] The particular mixture studied was a nearly 1:1 M mixture of BCl_3 and BBr_3 at 400 K. The spectrum for a mixing time of 50 ms is shown in Figure 21.4. Rate data were calculated by the three methods described in 21.2.2, with the direct matrix diagonalization method being preferred.

21.3.4 Silicon-29

Much insight into the silicate anion exchange pathways in ^{29}Si-enriched potassium silicate solutions has been gained by ^{29}Si EXSY.[38] Four intermolecular exchanges were discovered, involving monomeric anion, dimer, linear trimer, linear tetramer, and substituted cyclic trimer species, plus two intramolecular exchanges. Although this was only a qualitative study, it demonstrates the power of 2D EXSY over its 1D counterpart.

21.3.5 Phosphorus-31

This nucleus is well suited to EXSY studies in view of its high receptivity, wide chemical shift range, and common absence of $^{31}P-^{31}P$ cross relaxation. Numerous studies have been reported, one example being the octahedral organo chromium(0) complexes $[Cr(CO)_2(CX)\{(MeO)_3P\}_3]$ (X = S, Se).[39] These stereochemically nonrigid complexes undergo rearrangements via trigonal-prismatic (Bailar) intermediates. The ^{31}P EXSY experiments were of the "accordion" type[32] (see 21.2.5), with the factor κ having a magnitude of 30.

21.3.6 Vanadium-51

Quantitative kinetic data on oligomerization reactions of vanadate in aqueous solutions has been provided by ^{51}V EXSY.[40] At pH 8.6, the EXSY spectrum

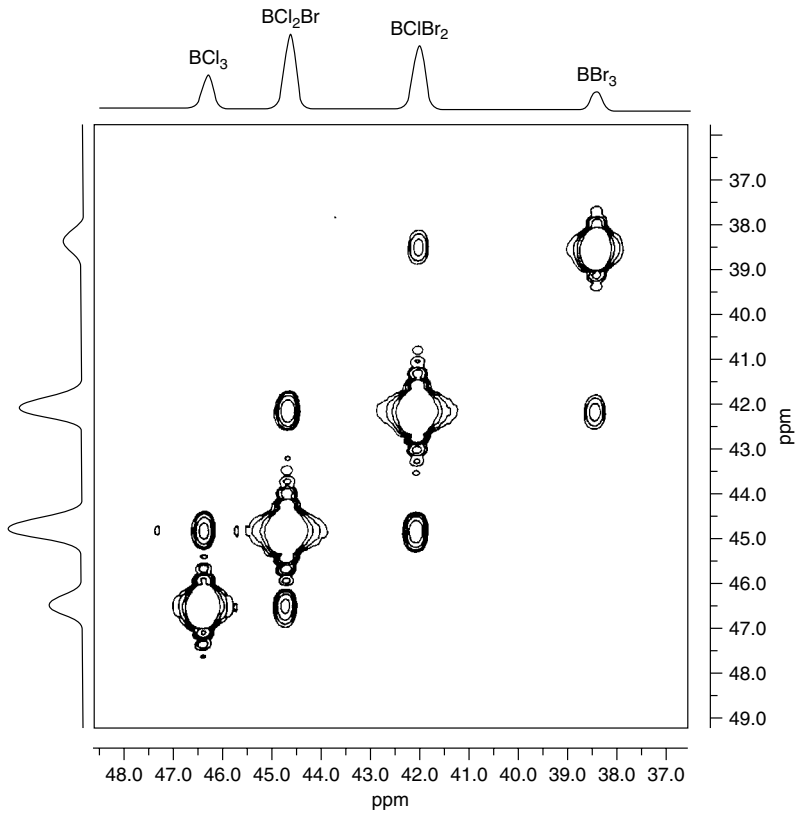

Figure 21.4. Boron-11 EXSY spectrum of a 1.05:1.0 M mixture of BCl_3 and BBr_3 at 400 K. The mixing time was 50 ms. The F_1 dimension contained 128 points, zero filled to 256 points. The F_2 dimension contained 512 real plus complex points. The number of scans per FID was 96.

shows all major oligomers, namely monomer, dimer, tetramer, and pentamer, exchanging with each other. Rates of several exchange pathways were identified. Mixing times were chosen in the range 8–10 ms.

21.3.7 Tin-119

The first example of ^{119}Sn EXSY was in connection with the dynamic stereochemistry of a ditin compound $CH_2[PhSn(SCH_2CH_2)_2NMe]_2$.[41] The spectrum, with a short mixing time of 5 ms, showed pairwise exchange of three isomers associated with uncorrelated isomerization of each tin centre. The same research group has also investigated $[MeSn(CH_2CH_2CH_2)_2NMe]_2$, which in solution exists as at least three isomers, two of which interconvert at rates measurable by ^{119}Sn EXSY.[42] See also Chapter 28.

21.3.8 Tellurium-125

Platinum(IV) complexes of the type $[PtXMe_3\{MeE(CH_2)_n\text{-}EMe\}]$ (E = S, Se, Te; X = Cl, Br, I; $n = 2$, 3) undergo a variety of internal rearrangements, the most facile being pyramidal inversion of the coordinated chalcogen atoms. When the chalcogen, E, is Se or Te, the inversion process can in theory be followed by ^{1}H, ^{13}C, ^{77}Se, ^{125}Te, and ^{195}Pt spectra. To avoid any complications from cross-relaxation effects, the rare nuclei are the preferred probes. The inversion process causes exchange between four isomers according to Scheme 21.1.

For the complex $[PtIMe_3\{MeTe(CH_2)_3TeMe\}]$, the Te inversion rates were measured by ^{125}Te EXSY.[43] Cross peaks were detected between the DL and *meso* signals only, indicating that rates of synchronous inversion of both Te atoms are negligible.

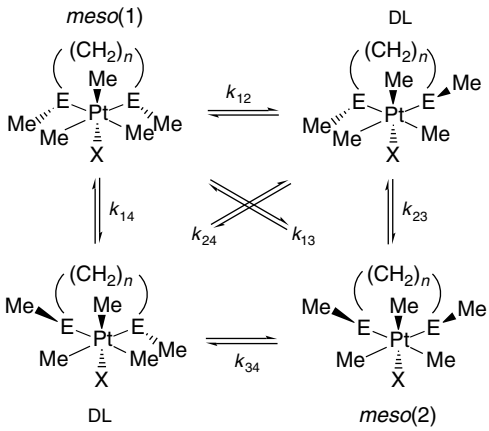

Scheme 21.1.

21.3.9 Platinum-195

^{195}Pt EXSY experiments are particularly powerful in monitoring exchange rates in the above Pt(IV) complexes. The EXSY spectrum of [$PtIMe_3(MeSCH_2CH_2SMe)$] is illustrated in Figure 21.5. The three isomers are identified as shown, the signals due to DL and *meso*(1) also possessing ^{13}C satellites. For the chosen mixing time of 0.3 s, cross peaks were detected between all three species. The inversion process is strictly represented by a four-site exchange problem (Scheme 21.1), but, when monitored by ^{195}Pt nuclei, it reduces to a three-site exchange since the DL pair are indistinguishable. Signal intensity data from the spectra were used to set up the intensity matrix $\boldsymbol{I}$ as defined earlier,[19] and the relative populations of the isomers enabled the matrix $\boldsymbol{P}$ to be constructed. The matrix conversion program[19] then generated the kinetic-plus-relaxation matrix $\boldsymbol{L}$, the off-diagonal elements of which provided rate constant magnitudes, namely, $k_{12} = 0.52 \pm 0.03\ s^{-1}$, $k_{23} = 0.50 \pm 0.03\ s^{-1}$, and $k_{13} = 0.004 \pm 0.04\ s^{-1}$. This latter rate constant for synchronous double inversion of both sulfur atoms is clearly zero within experimental uncertainty, despite the appearance of weak cross peaks I_{13} and I_{31}. This illustrates the point made earlier (see 21.2.2) that the existence of a cross peak does not necessarily imply direct exchange between the two sites in question, and so qualitative interpretations of EXSY spectra must be made with considerable caution. The same research group has studied the sulfur inversion dynamics of [$PtIMe_3(MeSCH_2CH_2SEt)$].[44] This constitutes a four-site exchange problem, a case too complex to be analyzed by total bandshape analysis. In contrast, the ^{195}Pt EXSY spectrum provided definitive rate data for the six distinct inversion pathways.

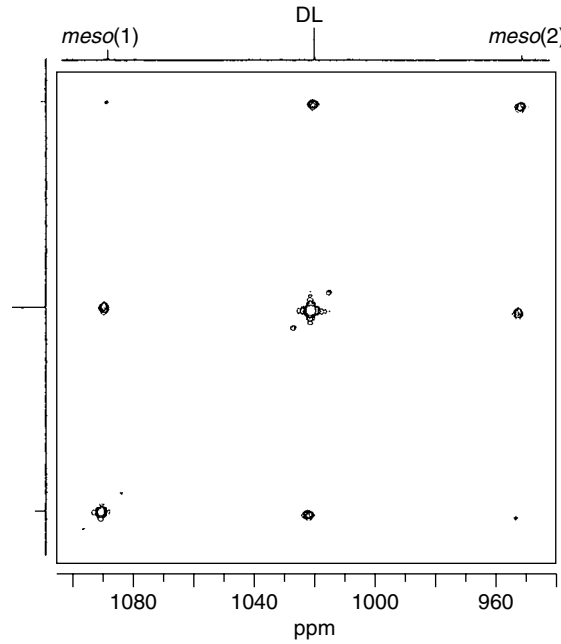

Figure 21.5. Platinum-195 EXSY spectrum of [$PtIMe_3(MeSCH_2CH_2SMe)$] at 253 K. The mixing time was 300 ms. The F_1 dimension contained 256 points, zero filled to 512 points. The F_2 dimension contained 1024 points.

RELATED ARTICLES IN THE ENCYCLOPEDIA OF MAGNETIC RESONANCE

Chemical Exchange Effects on Spectra

Double Resonance

Fluxional Motion

Inorganic Chemistry Applications

Organometallic Compounds

Relaxation Processes: Cross Correlation and Interference Terms

Selective Pulses

REFERENCES

1. H. S. Gutowsky and C. H. Holm, *J. Chem. Phys.*, 1956, **25**, 1228.
2. S. Forsén and R. A. Hoffman, *J. Chem. Phys.*, 1963, **39**, 2892; *J. Chem. Phys.*, 1964, **40**, 1189.
3. R. A. Hoffman and S. Forsén, *J. Chem. Phys.*, 1966, **45**, 2049.
4. J. J. Led and H. Gesmar, *J. Magn. Reson.*, 1982, **49**, 444.
5. H. Gesmar and J. J. Led, *J. Magn. Reson.*, 1986, **68**, 95.
6. R. Benn and H. Gunther, *Angew. Chem., Int. Ed. Engl.*, 1983, **22**, 350.
7. H. Kessler, M. Gehrke, and C. Griesinger, *Angew. Chem., Int. Ed. Engl.*, 1988, **27**, 490.
8. R. R. Ernst, G. Bodenhausen, and A. Wokaun, *Principles of Nuclear Magnetic Resonance in One and Two Dimensions*, Clarendon Press, Oxford, 1987, Chaps. 6–9.
9. D. Neuhaus and M. Williamson, *The Nuclear Overhauser Effect in Structural and Conformational Analysis*, VCH, New York, 1989.
10. J. Jeener, B. H. Meier, P. Bachmann, and R. R. Ernst, *J. Chem. Phys.*, 1979, **71**, 4546.
11. S. Macura and R. R. Ernst, *Mol. Phys.*, 1980, **41**, 95.
12. R. Willem, in *Progress in Nuclear Magnetic Resonance Spectroscopy*, ed. J. W. Emsley, J. Feeney, and L. H. Sutcliffe, Pergamon Press, Oxford, 1987, Vol. 20, p. 1.
13. C. L. Perrin and T. J. Dwyer, *Chem. Rev.*, 1990, **90**, 935.
14. K. G. Orrell, V. Šik, and D. Stephenson, in *Progress in Nuclear Magnetic Resonance Spectroscopy*, ed. J. W. Emsley, J. Feeney, and L. H. Sutcliffe, Pergamon Press, Oxford, 1990, Vol. 22, p. 141.
15. K. G. Orrell and V. Šik, in *Annual Reports on NMR Spectroscopy*, ed. G. A. Webb, Academic Press, London, 1993, Vol. 27, p. 103.
16. A. Kumar, G. Wagner, R. R. Ernst, and K. Wüthrich, *J. Am. Chem. Soc.*, 1981, **103**, 3654.
17. G. E. Hawkes, L. Y. Lian, E. W. Randall, K. D. Sales, and S. Aime, *J. Magn. Reson.*, 1985, **65**, 173.
18. C. L. Perrin and R. K. Gipe, *J. Am. Chem. Soc.*, 1984, **106**, 4036.
19. E. W. Abel, T. P. J. Coston, K. G. Orrell, V. Šik, and D. Stephenson, *J. Magn. Reson.*, 1986, **70**, 34.
20. E. R. Johnston, M. J. Dellwo, and J. Hendrix, *J. Magn. Reson.*, 1986, **66**, 399.
21. P. W. Kuchel, B. T. Bulliman, B. E. Chapman, and G. L. Mendz, *J. Magn. Reson.*, 1988, **76**, 136.
22. C. L. Perrin and R. E. Engler, *J. Magn. Reson.*, 1990, **90**, 363.
23. G. Wagner, G. Bodenhausen, N. Muller, M. Rance, O. W. Sorensen, R. R. Ernst, and K. Wuthrich, *J. Am. Chem. Soc.*, 1985, **107**, 6440.
24. J. Fejzo, W. M. Westler, S. Macura, and J. L. Markley, *J. Magn. Reson.*, 1991, **92**, 20.
25. C. T. W. Moonen, P. Van Gelderen, G. W. Vuister, and P. C. M. Van Zijl, *J. Magn. Reson.*, 1992, **97**, 419.
26. S. Davies, J. Friedrich, and R. Freeman, *J. Magn. Reson.*, 1987, **75**, 540.
27. Yu E. Chernysh, G. S. Borodkin, E. V. Sukholenko, and L. E. Nivorozhkin, *J. Magn. Reson.*, 1992, **96**, 131.
28. G. A. Morris and R. A. Freeman, *J. Magn. Reson.*, 1978, **29**, 433.
29. R. E. Engler, E. R. Johnston, and C. G. Wade, *J. Magn. Reson.*, 1988, **77**, 377.
30. B. T. Bulliman, P. W. Kuchel, and B. E. Chapman, *J. Magn. Reson.*, 1989, **82**, 131.
31. J. Jeener, *J. Chem. Phys.*, 1989, **90**, 2959.
32. G. Bodenhausen and R. R. Ernst, *J. Am. Chem. Soc.*, 1982, **104**, 1304.
33. C. Griesinger, O. W. Sorensen, and R. R. Ernst, *J. Magn. Reson.*, 1989, **84**, 14.
34. T. Beringhelli, G. D'Alfonso, H. Molinari, G. E. Hawkes, and K. D. Sales, *J. Magn. Reson.*, 1988, **80**, 45.
35. E. W. Abel, K. G. Orrell, K. B. Qureshi, V. Šik, and D. Stephenson, *J. Organomet. Chem.*, 1988, **353**, 337.
36. K. M. Briere, H. D. Dettman, and C. Detellier, *J. Magn. Reson.*, 1991, **94**, 600.
37. E. F. Derose, J. Castillo, D. Saulys, and J. Morrison, *J. Magn. Reson.*, 1991, **93**, 347.
38. C. T. G. Knight, R. J. Kirkpatrick, and E. Oldfield, *J. Magn. Reson.*, 1988, **78**, 31.
39. A. A. Ismail, F. Sauriol, and I. S. Butler, *Inorg. Chem.*, 1989, **28**, 1007.
40. D. C. Crans, C. D. Rithner, and L. A. Theisen, *J. Am. Chem. Soc.*, 1990, **112**, 2901.

41. C. Wynants, G. Van Binst, C. Muegge, K. Jurkschat, A. Tzschach, H. Pepermans, M. Gielen, and R. Willem, *Organometallics*, 1985, **4**, 1906.

42. K. Jurkschat, A. Tzschach, C. Muegge, J. Piret-Meunier, M. Van Meerssche, G. Van Binst, C. Wynants, M. Gielen, and R. Willem, *Organometallics*, 1988, **7**, 593.

43. E. W. Abel, K. G. Orrell, S. P. Scanlon, D. Stephenson, T. Kemmitt, and W. Levason, *J. Chem. Soc., Dalton Trans.*, 1991, 591.

44. E. W. Abel, I. Moss, K. G. Orrell, V. Šik, and D. Stephenson, *J. Chem. Soc., Dalton Trans.*, 1987, 2695.